2023 IEEE International Conference on Robotics and Automation (ICRA 2023)
May 29 - June 2, 2023. London, UK

Stable Station Keeping of Autonomous Sailing Robots via the Switched Systems Approach for Ocean Observation

Weimin Qi[1], Qinbo Sun[1], Yu Cao[2] and Huihuan Qian[1,†]

***Abstract*— Ocean observation is an emerging field, and sailing robots have several promising features (e.g., long-range sailing, environmental friendliness, energy-saving and low-noise) to perform tasks. In this paper, we define an ocean observation mission in a restricted target area as a station keeping problem. Inspired by an orientation-restricted Dubins path method, the robot keeps sailing and collecting data in a smooth reciprocation, where the trajectories consist of sailing against wind segments and turning downwind parts divided by a goal area and an acceptable area. The upwind sailing segments are of interest for data acquisition. However, the system stability can not be guaranteed during the whole reciprocation especially for sailing outside the goal area. Hereby, we refer to a switched systems approach and propose a desired heading generation scheme to realize safe and stable control in both areas. The stability for subsystems is proved with Lyapunov-like functions. The stable station keeping scheme is verified in both simulation and real experiments. Finally, we completed continuous and effective observation within 50 minutes in the goal area with a radius of 50 meters by a catamaran robot named OceanVoy460.**

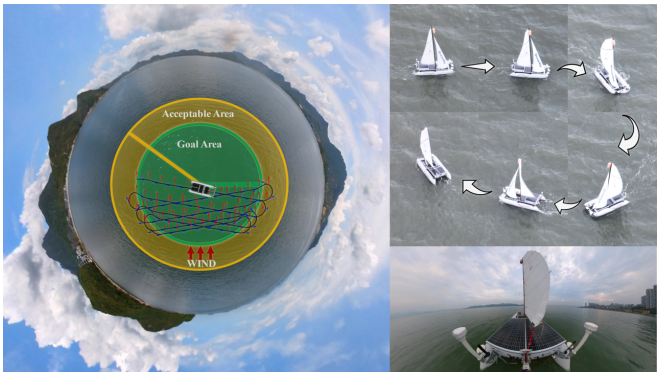

Fig. 1. Overview of the stable station keeping scheme. (Left) Panoramic view of specified ocean area to be monitored, in which the sailing robots should sail smoothly and collect valid data. The area in green is the goal area for observation. Sailing in yellow area is still acceptable. Reciprocation trajectories are contained in blue. (Right top) An example of jibing (turning downwind), and the wind is blowing from the top. (Right bottom) A wide-angle view of OceanVoy460.

I. Introduction

Station keeping is the act of maintaining balance in a specified position even when disturbed [1]. It is an indispensable navigational behaviour for marine robots especially in tasks such as environmental observation [2], [3], virtual moorings [4] and research on marine hydrodynamics [5]. Sailing robots [6] such as Sailbuoy [7], [8] and Saildrone [9], [10] are superior in long-term ocean observation profit from the environmentally benign characteristic and ability to survive for a long time. Compared with the underwater marine robots, which are mainly affected by the hydrodynamic field when maintaining the station [11], [12], the surface marine robots including sailing robots also need to deal with the influence of the aerodynamic field [13], [14], [15]. Moreover, sailing robots are propelled by wind rather than stable and controllable power like electricity or fuel oil. Therefore, maintaining the station of a sailing robot is a great challenge.

Predecessors have made some exploration on the station keeping task of sailboats. Station Keeping Autonomous Mobile Platform (SKAMP) was an early mobile surveillance platform that relied on wind to propel its curved ring wing sail to realize station keeping [16], [17]. However, there is little information about its station keeping control strategy or performance. Atlantis [18], [19], a wing sail catamaran, kept station via a waypoints-based guidance strategy. However, the implementation relied on assistance from motors.

Then, another method was proposed to help a sailboat reach and stay at a stationary target position by adjusting the sailboat heading into the no-go zone [20]. The no-go zone is a certain range of orientations that the sailboat cannot reach [21]. This station keeping scheme was validated in simulation. However, in the real ocean, the low-speed sailing toward the no-go zone will pose a threat to safety because the controllability of the sailboat is reduced. Specifically, sailboats cannot avoid obstacles in time or even illegally occupy channels. Based on the control strategy of [20], a station keeping method depended on tacking and wearing maneuvers was investigated [22]. However, stall problems still occurred during tacking, which may be caused by insufficient speed before turning or lacking power due to improper sail trim. Therefore, the afore-mentioned two methods can not effectively ensure the safety due to the stall problem.

Nowadays, robotic sailing has a few interesting competitions e.g., the International Robotic Sailing Regatta (SailBot) [23], World Robotic Sailing Championships (WRSC) [24] and Microtransat Challenge [25]. Station keeping is also continuously practiced as a kind of competition item. This event began to appear on the score sheet of SailBot in 2008. In WRSC, it has been defined as autonomous navigation within a given area for a period since 2012. In the realm

*This paper is partially supported by Project U1813217 and U1613226 from NSFC, Project AC01202101105 from the Shenzhen Institute of Artificial Intelligence and Robotics for Society, and University Stability Support Program from Shenzhen Natural Science Foundation, Shenzhen, China.

[1]Shenzhen Institute of Artificial Intelligent and Robotics for Society, The Chinese University of Hong Kong, Shenzhen, Guangdong, China.
[2]Huawei Technologies Co., Ltd, Shenzhen, Guangdong, China.
† Corresponding author is Huihuan Qian, hhqian@cuhk.edu.cn

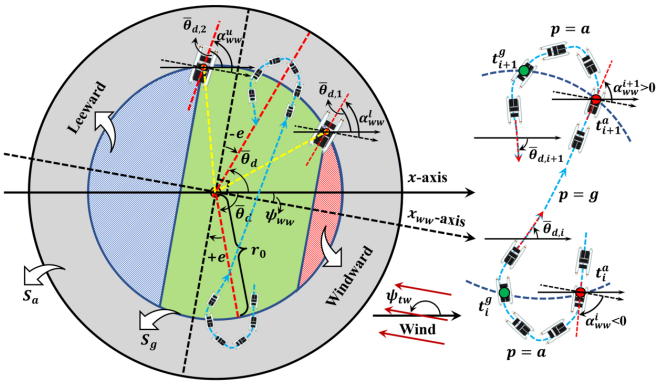

Fig. 2. Illustration of symbols and Algorithm 1. The region in blue circle is the goal area S_g and the region in gray ring is the acceptable area S_a. r_0 is the radius of S_g. x axis is in the world coordinate toward east. x_{ww} in dotted black line is the axis opposite the wind direction. The red dotted lines represent the desired heading angles. The blue and red shadowed regions are the leeward zone and windward zone, respectively. The green region is the expected sailing zone. These three zones can be rotated according to the true wind ψ_{tw}. The yellow dotted lines pointed to the azimuth lower bound α^l_{ww} and upper bound α^u_{ww} with respect to x_{ww} axis. $\bar{\theta}_d$ represents the desired heading angle. $\bar{\theta}_{d,i}$ and $\bar{\theta}_{d,i+1}$ are generated desired heading angles during periods of t^a_i to t^g_i and t^a_{i+1} to t^g_{i+1}, respectively.

of racing, the quest for station keeping is continuing.

We expect the sailing robot to realize long-duration data collection in a designated sea area. Inspired by a station keeping scheme based on an orientation-restricted Dubins path approach [26], we aim to keep safe and stable sailing in smooth trajectories as shown in Fig.1. In our experience, sailing against the wind is better for data acquisition than turning. Therefore, to effectively complete the observation objective, we define an acceptable area as a turning buffer on the periphery of the target area. In two areas, we refer to the switched systems approach [27] to realize stable reciprocation keeping. During the entire sailing process, we collect and record ocean data including sailboat pose, wind field, water speed, temperature, humidity, magnetic flux, different field of view videos, etc. Our strategy has been validated in both simulations and experiments.

The rest of this paper is structured as follows. Section II elaborates the goal and a sketch of a solution. Section III shows the switched systems based control scheme. Section IV introduces the simulation. Section V shows the experimental results. Section VI concludes the study.

II. Problem Description

Toward ocean observation, our goal is to collect valid data by reciprocating smoothly in the goal area. It is inspired by the orientation-restricted Dubins path method in [26]. The trajectories consist of segments sailing against the wind and turning downwind. During turning, the speed and motion trend of the sailboat change. Compared to the turning process, there is no sudden change in speed and attitudes while sailing against the wind. Hereby, data collection during the straight sailing period is more stable and realistic than turning. For example, velocity fluctuations and heading reversals that occur during a turn can affect the performance of the water flow sensor. Therefore, in the whole monitoring process, it is desirable for the vessel to spent the majority of time sailing against the wind within the goal area. Meanwhile, the reciprocation sailing strategy is also beneficial to ensure safety. There is no sudden stall at any stage of sailing, so the speed of the sailboat is large enough to maintain its risk-avoiding maneuverability. The avoidance task is not the focus of this paper, but schemes we have completed before can be referenced [28].

The robot switches to sail between the goal area S_g and acceptable area S_a as shown in Fig.2. S_a is located on the periphery of S_g for turning and preparing the next upwind section. ∂S_g is the acceptable boundary between S_g and S_a. Sailing outside the forbidden boundary ∂S_a is not allowed.

When the sailboat sails out of S_g, it should return safely and stably by turning downwind. However, during this procedure, the system stability is not verified. We refer to control policies using a switched systems approach [27] because they are appropriate to our problem. The stability of subsystems is proved with Lyapunov-like functions. During the whole reciprocation, we control the sailing robot according to the desired heading state. Dwell time constraints of subsystems act as stability conditions of the whole system, which need to be satisfied for switching processes. Thereby, sailing stability between S_g and S_a can be ensured.

Moreover, the dwell time during sailing in S_a can be used as the basis for safety judgment. If the time exceeds a set maximum time threshold, the sailing status is abnormal such as a grounding, off-course or collision.

III. Methodology

As mentioned in Section II, we convert the stable station keeping problem to a heading tracking problem. Switched systems can track the desired heading state with guaranteed Lyapunov-like stability. Consequently, we propose a scheme to generate the desired heading. Specifically, the control law is updated according to the desired heading and then acts on the dynamic model of the sailboat.

A. Switched Systems for the Tracking Problem

We refer to the switched systems method in [27] and modify it to track the heading state. A dynamic system is

$$\dot{\mathbf{x}}(t) = f(\mathbf{x}(t), t) + u(t) + d(t) \tag{1}$$

where $\mathbf{x}(t) \in \mathbb{R}^n$ is the system state. f denotes the locally Lipschitz drift dynamics. $u(t)$ is the control input. $d(t)$ is the disturbance and $\|d(t)\| \leq \bar{d} \in \mathbb{R}_{\geq 0}$.

We set subsystems in S_g and S_a as $p = g$ or $p = a$ as shown in the right part of Fig.2. $\bar{\mathbf{x}}_d(t)$ is a sequence of desired heading $\bar{\theta}_d(t)$. Following $\bar{\mathbf{x}}_d(t)$, the whole system should satisfy dwell time constraints. The dwell times for the $p = g$ and $p = a$ cases are $\Delta t^g_i \triangleq t^a_i - t^g_i \in \mathbb{R}_{>0}$ and $\Delta t^a_i \triangleq t^a_{i+1} - t^a_i \in \mathbb{R}_{>0}$. The estimate tracking error $e_1(t)$ and the state estimation error $e_2(t)$ related to heading states $\theta(t)$ and heading estimates $\hat{\theta}(t)$ are

$$\begin{cases} e_1(t) \triangleq \hat{\theta}(t) - \bar{\theta}_d(t) \\ e_2(t) \triangleq \theta(t) - \hat{\theta}(t) \end{cases} \tag{2}$$

Then, the tracking error is $z(t) \triangleq \begin{bmatrix} e_1^T(t) & e_2^T(t) \end{bmatrix}^T$.

The designed controller is

$$u(t) = \begin{cases} \dot{\bar{\theta}}_d(t) - f(\hat{x}(t), t) - k_1 e_1(t) - u_r(t), & p = g \\ \dot{\bar{\theta}}_d(t) - f(\hat{x}(t), t) - k_1 e_1(t) & p = a \end{cases} \tag{3}$$

where $u_r(t) = k_2 e_2(t) + \bar{d}\,\mathrm{sign}(e_2(t))$. k_1 and k_2 are gain parameters for $e_1(t)$ and $e_2(t)$.

For switched systems, a Lyapunov-like function is

$$V_\sigma(z(t)) = V_1(e_1(t)) + V_2(e_2(t)) \tag{4}$$

where the candidate Lyapunov functions are $V_1(e_1(t)) = \frac{1}{2} e_1^T(t) e_1(t)$ and $V_2(e_2(t)) = \frac{1}{2} e_2^T(t) e_2(t)$.

Therefore, the stability of state transition between $p = g$ and $p = a$ requires that $V_\sigma(z(t))$ is always less than or equal to the following corresponding conditions

$$\begin{cases} V_\sigma\left(z\left(t_i^g\right)\right) e^{-\lambda_s\left(t - t_i^g\right)}, t \in \left[t_i^g, t_i^a\right) \\ V_\sigma\left(z\left(t_i^a\right)\right) e^{\lambda_u\left(t - t_i^a\right)} - \frac{\bar{d}^2}{2\lambda_u}\left(1 - e^{\lambda_u\left(t - t_i^a\right)}\right), t \in \left[t_i^a, t_{i+1}^g\right) \end{cases} \tag{5}$$

which is globally exponentially convergent in S_g and exponentially growing in S_a. λ_s and λ_u are subsequently defined as known positive constants. Hereby, the dwell time conditions in S_g and S_a are

$$\begin{cases} \Delta t_i^g \geq \frac{-1}{\lambda_s} \ln\left(\min\left(\frac{V_T}{V_\sigma\left(z\left(t_i^g\right)\right)}, 1\right)\right) \\ \Delta t_i^a \leq \frac{1}{\lambda_u} \ln\left(\frac{V_M + \frac{\bar{d}^2}{2\lambda_u}}{V_\sigma\left(z\left(t_i^a\right)\right) + \frac{\bar{d}^2}{2\lambda_u}}\right) \end{cases} \tag{6}$$

V_M, V_T are maximum, minimum thresholds on $V_\sigma(z(t))$.

B. Desired Heading Generation Scheme

Entering the no-go zone will cause the sailboat to lose effective propulsion and be unsafe and unstable. Worse yet, catamarans have a larger no-go zone than monohull sailboats. Therefore, avoiding no-go zones is important and challenging for the catamaran. In this problem, under the no-go zone constraint, the desired heading should be obtained according to phases in S_g and S_a, respectively.

1) $p = g$: Sailing Against the Wind: In the marine environment, there is typically no sudden change of wind direction over a period of time. Therefore, sailboats can choose to sail when the wind field is stable to keep smooth sailing. The proper desired heading state is obtained based on the true wind direction.

2) $p = a$: Turning Downwind: The goal is to return from S_a to S_g. Jibing and tacking are available to achieve this. However, the tacking process will cross the no-go zone and cause a stall. Thus, the jibing method is suitable. Hereby, the desired heading state should be the next stage of $p = g$.

3) Desired Heading Generation: As shown in Fig.2 and Algorithm 1, we propose a scheme to generate the desired heading sequence refer to the center (x_0, y_0), real-time position (x, y), wind direction (ψ_{tw}) and the radius r_0 of S_g. The distance r and azimuth α_x between sailboat and center is calculated in Line1 and Line3, respectively. In Fig.2, x_{ww} axis points to the direction opposite to the true wind and toward the windward zone. The angle between x axis and x_{ww} axis is denoted by ψ_{ww} and obtained from Line2. $diff$ function is used to rotate α_x to ψ_{ww}. Hereby, α_{ww} determines how far the sailboat approaches the windward zone. The desired heading $\bar{\theta}_d$ is initialized by an orthogonal direction of ψ_{ww}. The direction is chosen in Line5.

Line6 to Line11 is the case where the sailboat sails from

Algorithm 1 Function $\bar{\theta}_d(x, y, \theta, \psi_{tw}, x_0, y_0, r_0)$

1: $r = ||(x, y) - (x_0, y_0)||$;
2: ψ_{ww} : the reversed direction of true wind ψ_{tw};
3: $\alpha_x = atan2(y - y_0, x - x_0)$;
4: $\alpha_{ww} = diff(\alpha_x, \psi_{ww})$;
5: $\bar{\theta}_d = \arg\min_{\theta_0}(\theta - \theta_0)$, where $\theta_0 = \psi_{ww} \pm (\pi/2)$
6: **if** $r > r_0$ **and** $\alpha_{ww} > 0$ **then**
7: //$p = a$: jibing (from starboard to port)
8: $\bar{\theta}_d = \psi_{ww} + (-\pi/2 + e)$;
9: **else if** $r > r_0$ **and** $\alpha_{ww} < 0$ **then**
10: //$p = a$: jibing (from port to starboard)
11: $\bar{\theta}_d = \psi_{ww} + (\pi/2 - e)$;
12: **else if** $r \leq r_0$ **then**
13: //$p = g$: sailing against the wind
14: Using $\bar{\theta}_d$ same with line8 or line11;
15: **end if**
16: **if** $r > r_0$ **and** $|\alpha_{ww}| <= \alpha_{ww}^l$ **then**
17: //Do once: decrease e to increase $|\alpha_{ww}|$
18: $e = e - k_e$
19: **else if** $r > r_0$ **and** $|\alpha_{ww}| > \alpha_{ww}^u$ **then**
20: //Do once: increase e to decrease $|\alpha_{ww}|$
21: $e = e + k_e$
22: **end if**
23: **return** $\bar{\theta}_d$

TABLE I
PARAMETERS AND CORRESPONDING VALUES OF SAILBOAT MODEL

Parameter	Value	Parameter	Value
p1: Drift Coefficient (Coef)	0.03	p7: Distance to Mast	0.5
p2: Tangential friction	270	p8: Distance to Rudder	2
p3: Angular friction	3500	p9: Mass of the boat	300
p4: Sail lift	450	p10: Moment of inertia	5000
p5: Rudder lift	650	p11: Rudder break Coef	0.08
p6: Distance to Sail CoE	0.5		

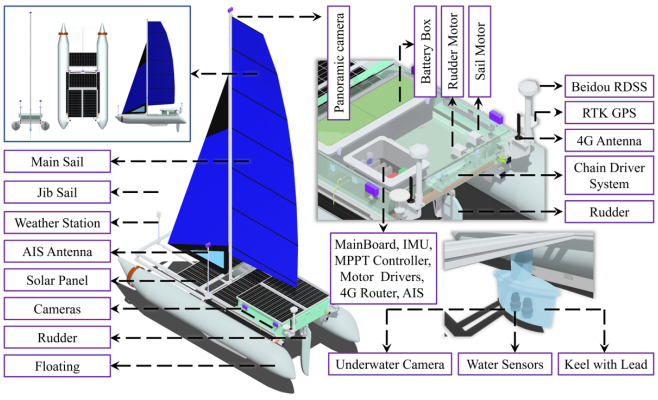

Fig. 3. Hardware design and sensors deployment of OceanVoy460.

S_g to S_a corresponding to the $p = a$ process. The jibing direction is different for turns as shown in Line8 and Line11. In this process, e is used to control the heading angle.

Line12 to Line14 represents the scenario where $p = g$. The updated $\bar{\theta}_d$ in phase $p = a$ will be kept. Otherwise, the initialized $\bar{\theta}_d$ can be used.

Line16 to Line21 is used to keep the sailboat close to or away from the windward direction as shown in Fig.2. It is not advisable to get too close due to the shortened distance of phase $p = g$. Meanwhile, being too far away may sail out of the goal area. Hereby, we wish to keep sailing in green area. k_e is used to control the α_{ww} in the range $(\alpha^l_{ww}, \alpha^u_{ww})$.

C. Dynamic Model of Sailboat

The dynamic model of the sailboat is inspired by [29]. It is a simplified model considering position (x, y), heading angle θ, linear velocity v and angular velocity ω,

$$\begin{cases} \dot{x} = v\cos(\theta) + p_1 a_{tw}\cos(\psi_{tw}) \\ \dot{y} = v\sin(\theta) + p_1 a_{tw}\sin(\psi_{tw}) \\ \dot{\theta} = w \\ \dot{v} = \frac{g_s \sin(\delta_s) - g_r p_{11}\sin(\delta_r) - p_2 v^2}{p_9} \\ \dot{w} = \frac{g_s(p_6 - p_7\cos(\delta_s)) - g_r p_8\cos(\delta_r) - p_3 wv}{p_{10}} \end{cases} \tag{7}$$

where $g_s = p_4 a_{aw}\sin(\delta_s - \psi_{aw})$, $g_r = p_5 v^2 \sin(\delta_r)$. δ_s and δ_r are sail angle and rudder angle, respectively. a_{tw} and ψ_{tw} are speed and direction of the true wind. a_{aw} and ψ_{aw} refer to the apparent wind speed and direction. If e is increased, the desired heading will be windward and the a_{ww} will decrease, and vise versa. We updated the model based on the parameters of the OceanVoy460 sailboat as shown in Fig.3. The parameters and their values in simulation can be found in Table.I.

D. Low-level Controller

For low-level control of the sailboat, we decouple the rudder and sail control to simply the control problem. The rudder controller is designed in equation (3) for heading tracking, and the sail controller refers to the method we implemented in [30].

IV. Simulation

We simulated the proposed stable station keeping scheme in MATLAB. We consider implementing the simulation with a stable wind angle $\psi_{tw} = \pi$. The area center is $(0, 50)$ and the radius r_0 is $50m$. Parameters k_1, k_2, k_e and $\bar{d}$ are set as 0.5, 0.5, 0.05 and 0.035. The range for α_{ww} is $(0.3, 2*\pi/3)$. V_M and V_T are given as 0.45 and 0.1. The initial state for $[x, y, \theta, v, \omega]$ is $[-5, 0, \pi/2, 0.1, 0]$.

We designed two simulation cases. Within the expected sailing zone, the coverage area can be adjusted according to the ocean observation mission. Fig.4 shows trajectories, real-time desired heading and simulated heading, error and value for stability functions.

1) Sim1: The sailboat sails against the wind approaching windward zone as shown in Fig.4(a) to Fig.4(c). In Fig.4(a), the red arrows represent the true wind field, which is stable over the case. The sailboat starts at point (-5,0). The desired

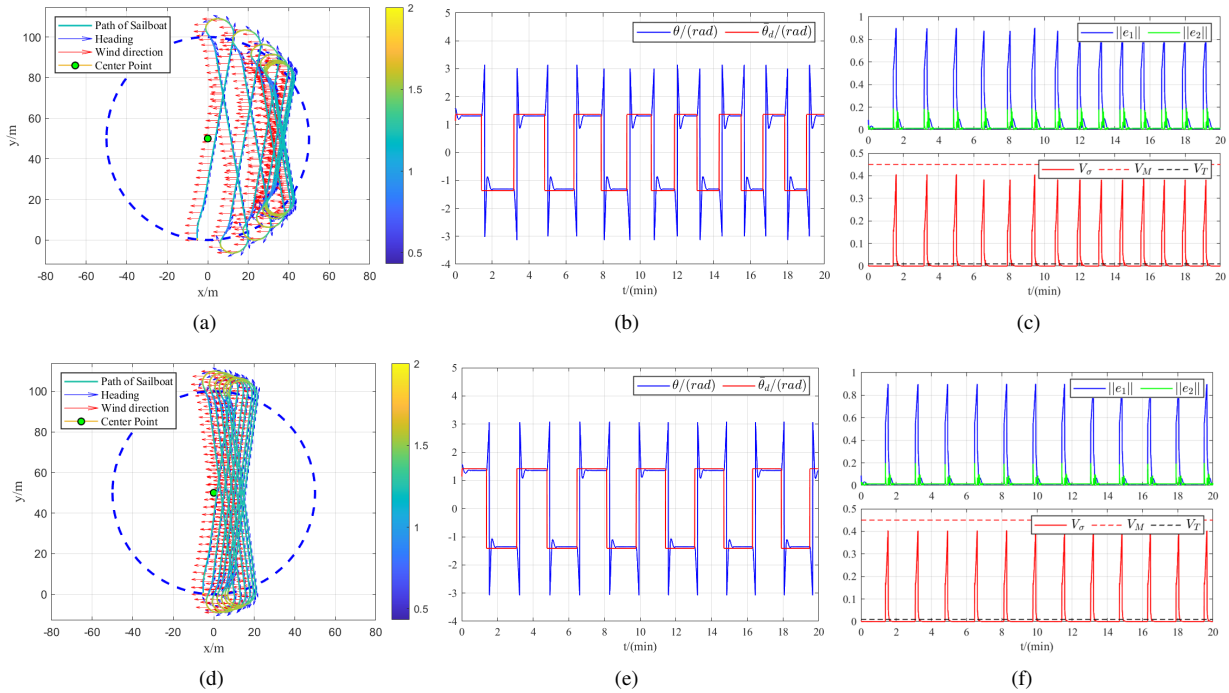

Fig. 4. Simulation results: (a)-(c) and (d)-(f) are corresponding to Sim1 and Sim2, respectively. In (a) and (d), the wind blows from the east (right side) and the sailboat sails with reciprocation trajectories. Wind velocity is marked along the trajectory with red arrows, the length of arrows reflects the magnitude of wind speed. Green circles are centers of the target area in Cartesian coordinates. The sailboat speed (m/s) is shown in the color map. The warmth of the color corresponds to the magnitude of the speed. Blue arrows represent sailboat heading angle. (b) and (e) show the desired heading in red and simulated heading in blue in time series. (c) and (f) show the norm of the estimate tracking heading error e_1 in blue, the norm of state estimation error e_2 in green and Lyapunov-like function value V_σ in red.

heading $\bar{\theta}_d$ is $\pm 1.36(rad)$. When it reaches the boundary ∂g, the control strategy in S_a is triggered to turn downwind by following $\bar{\theta}_d$. The overall sailing area is approaching the windward zone. When the lower bound α^l_{ww} is reached, $\bar{\theta}_d$ will be tuned slightly by parameter k_e to move away from the windward area as mentioned in Line17 of Algorithm 1.

In Fig.4(b), the actual heading control is basically consistent as expected. In Fig.4(c), the norm of e_1 and e_2 increase rapidly when sailing in S_a and decrease to converge quickly in S_g. Combining e_1 and e_2, V_σ is bounded by V_M and V_T during the whole procedure so as to guarantee the stability of the system.

2) Sim2: The sailboat sails against the wind and keeps away from the windward zone as shown in Fig.4(d). In Fig.4(e), compared with Sim1, $\bar{\theta}_d$ is changed to $\pm 1.41(rad)$. Fig.4(f) shows that the system is stable during Sim2.

In Table.II, the maximum dwell time Δt^a_i in Sim1 and Sim2 is no more than $20.40s$. The average Δt^a_i in simulation is $15.05s$. According to equation (6), the upper bound for Δt^a_i is $25.69s$. Therefore, the stability condition of subsystem is satisfied in simulation.

V. Experiment

A. Experiment Set Up

OceanVoy460 is an autonomous catamaran sized by $4.6m \times 2.2m \times 6.1m$. The area of the jib sail and the main sail is $3.5m^2$ and $8.0m^2$, respectively. The designed payload is $450kg$ and the weight equipped with devices is $300kg$. It deploys a weather station, a set of Beidou RDSS, an AIS, a set of RTK-GPS, water sensors, cameras and solar panels with a total maximum power of $600W$. Batteries, electronics and motors are installed in different isolated boxes for waterproofing. Worm gears boxes and wheels are used to control the rudder and sail rope. We designed a glider and slider for the jib sail to change the direction automatically. To avoid capsizing in harsh conditions, we designed a keel to prevent the danger. Water sensors and underwater cameras are integrated into the keel.

We performed the experiments in the coastal sea near Daya Bay, China. The center of the goal area is located at (0, 50) and the radius is $50m$. Parameters k_1, k_2, k_e and $\bar{d}$ are given as 0.5, 0.5, 0.085 and 0.035. V_M and V_T are set as 0.7 and 0.1. OceanVoy460 is released in the goal area and sails against the wind with initialized desired heading.

B. Experimental Results

Two groups of results about sailing performance and environmental monitoring will be shown in this section. We performed Test1 and Test2 corresponding to Sim1 and Sim2.

1) Test1 and Test2: In Fig.5, experimental results of Test1 and Test2 are shown. It can be observed that the wind fields were stable during the respective tests. Results contain reciprocation trajectories, comparison between the true wind

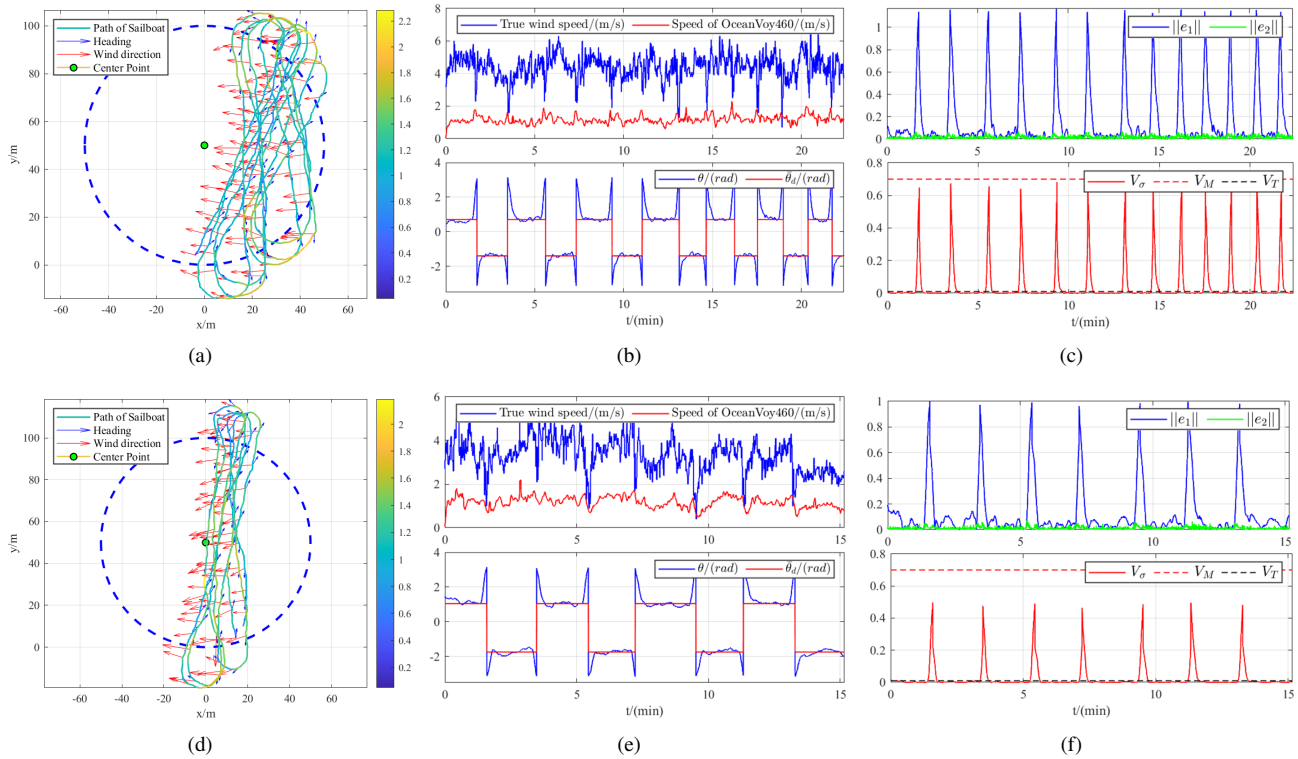

Fig. 5. Experiment results of Test1 and Test2 correspond to (a-c) and (d-f), respectively. (a) and (d) show the reciprocation trajectories of two tests. The wind is mainly from the east. Red arrows show the true wind information. Green circles are centers of target areas. The color of trajectories reflects the speed of the sailboat (m/s). Blue arrows represent sailboat heading angle. (b) and (e) show (upper) the comparison between true wind speed and sailboat speed and (bottom) trend comparison between the true heading and the desired heading. In (c) and (f), $\|e_1\|$ and $\|e_2\|$ are norm of the estimate tracking heading error e_1 in blue and state estimation error e_2 in green, and V_σ in red is value for Lyapunov-like stability function.

speed and OceanVoy speed, desired and real heading, errors and values of stability functions.

In Fig.5(a) and Fig.5(d), OceanVoy keeps sailing in reciprocation smoothly. In Fig.5(d), the sailboat sails further away from windward zone. In both tests, OceanVoy460 sails against the wind in S_g and turns in S_a. During turns, relatively large speed can still be maintained, which guarantees the safety. The sailboat sails upwind and ensures to collect data stably and effectively.

In the upper parts of Fig.5(b) and Fig.5(e), the speed of OceanVoy is about a third of the wind speed. OceanVoy's speed tends to change in a similar way as wind speed rises and falls. In the bottom parts, heading south upwind, the desired heading for Test1 is -1.40rad and that of Test2 is adjusted to -1.74rad. Heading north upwind, the desired heading for Test1 and Test2 are 0.70rad and 1.04rad. After encountering ∂g, OceanVoy can always turn back to S_g and continue to sail against the wind. Therefore, the effectiveness of the control systems is verified.

In Fig.5(c) and Fig.5(f), the norm of e_1 and e_2 are shown. The function of V_σ is bounded by the V_M during the test. Accordingly, the system works stably.

From Table.II, the maximum Δt_i^a in Test1 and Test2 is 39.97s. The average Δt_i^a in experiments is 30.70s. According to equation (6), the upper bound for Δt_i^a is 46.74s. Therefore, the stability of the system is guaranteed in experiments.

2) Observed ocean information: A continuous and stable station keeping over 50 minutes is showed in Fig.6(a). This is a period when the wind is mostly steady. However, the varied wind fields must be considered over long-term observation. Hereby, the speed of OceanVoy during upwind sailing and turning is sufficient to ensure controllability. In Fig.6(b) and Fig.6(c), under the premise of safety and stability, sensors collected the data of the ocean.

We obtained the position, heading angle, speed, angular velocity, sailing course and linear acceleration of the sailboat. Then real-time wind field, air and water temperature, air pressure and magnetic field along sailing trajectories were also collected. Images and videos captured from the surrounding cameras also provide meaningful information for ocean observation. In the future, we will add sensors to collect other data e.g. salinity and oxygen content.

VI. Conclusion

In this paper, we investigated stable station keeping and collected abundant data on the coastal ocean environment. The switched system and the proposed desired heading generation scheme guaranteed Lyapunov-like stability for sailing between the goal area and the acceptable area. The windward sailing segments, as the part of interest for data acquisition, are the dominant component of the trajectories as expected. The safety of the robot during sailing is also guaranteed. Both simulations and experiments have verified the feasibility and effectiveness of the stable station keeping scheme. Finally, observations lasting 50 minutes have been achieved in the goal area with a radius of 50m by OceanVoy460.

In the future, we will also study the influence factors such as tides, varied wind fields, energy consumption and turning radius on long-term observation. We've noticed in experiments that sailboats tend to drift in flood and ebb tides.

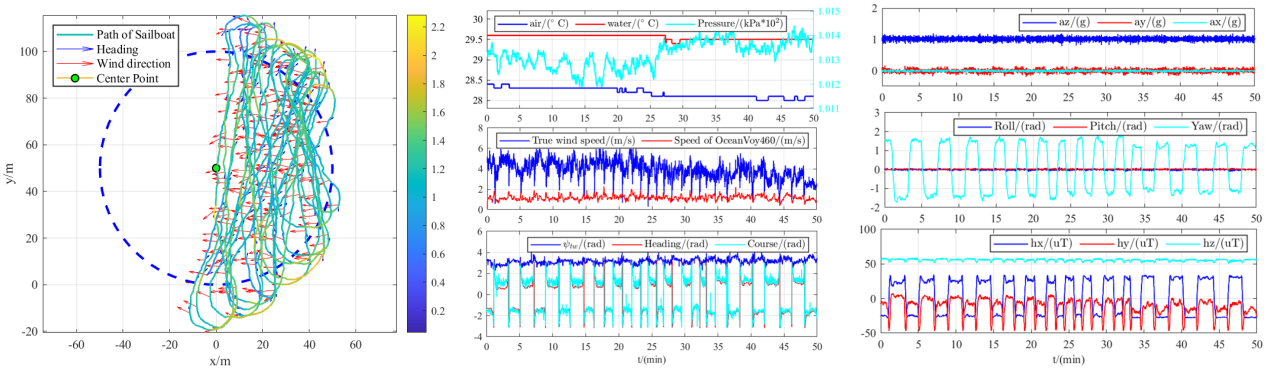

(a) (b) (c)

Fig. 6. Observed ocean information via OceanVoy460. (a) Continuous reciprocation trajectories of 50 minutes with a radius of 50m. (b) (top) Air temperature, water temperature, and air pressure at the real-time location of the sailboat. (middle) True wind speed and OceanVoy speed over the entire track. (bottom) The wind direction, heading and course of OceanVoy460. (c) (top) Linear acceleration of OceanVoy in x, y and z directions, and g is 9.8m/s^2. (middle) Attitude of the sailboat in roll, pitch and yaw directions. (bottom) Magnetic fields in the x, y, and z directions.

TABLE II

Dwell time Δt_i^a (s) of simulations and experiments

Turn	1	2	3	4	5	6	7	8	9	10	11	12
Sim1	20.40	17.40	15.60	13.80	12.60	12.00	11.40	10.80	10.80	10.80	10.80	10.20
Sim2	19.80	18.60	18.00	18.00	16.80	16.80	16.80	16.80	15.60	15.60	16.20	15.60
Test1	26.52	31.59	26.64	33.74	22.62	33.83	28.70	25.75	27.85	19.79	31.01	26.65
Test2	38.61	32.76	37.98	36.83	39.97	31.80	-	-	-	-	-	-

REFERENCES

[1] U. Nagarajan, G. Kantor, and R. Hollis, "The ballbot: An omnidirectional balancing mobile robot," *The International Journal of Robotics Research*, vol. 33, no. 6, pp. 917–930, 2014.

[2] H. Oh, S. Kim, A. Tsourdos, and A. Savvaris, "Comparison of station keeping strategies for long endurance autonomous surface vehicle," *Journal of Marine Science and Technology*, vol. 25, no. 1, pp. 13–25, 2020.

[3] Y. Fujii, K. Harada, H. Yamazoe, and J.-H. Lee, "Development and performance experiments in lake biwa of a small sensing device keeping fixed position on water," in *2020 17th International Conference on Ubiquitous Robots (UR)*. IEEE, 2020, pp. 494–499.

[4] T. I. R. S. R. (SailBot), "https://www.roboticsailing.org/2018/competition," 2018.

[5] D. C. Fernández and G. A. Hollinger, "Model predictive control for underwater robots in ocean waves," *IEEE Robotics and Automation letters*, vol. 2, no. 1, pp. 88–95, 2016.

[6] Q. Sun, W. Qi, H. Liu, X. Ji, and H. Qian, "Toward long-term sailing robots: State of the art from energy perspectives," *Frontiers in Robotics and AI*, vol. 8, 2021.

[7] M. H. Ghani, L. R. Hole, I. Fer, V. H. Kourafalou, N. Wienders, H. Kang, K. Drushka, and D. Peddie, "The sailbuoy remotely-controlled unmanned vessel: Measurements of near surface temperature, salinity and oxygen concentration in the northern gulf of mexico," *Methods in Oceanography*, vol. 10, pp. 104–121, 2014.

[8] R. S. Borge, "Application of the unmanned offshore sensing sailbuoy for validation of ocean model simulations and remote sensing data in the north atlantic," Master's thesis, The University of Bergen, 2015.

[9] F. Chai, K. S. Johnson, H. Claustre, X. Xing, Y. Wang, E. Boss, S. Riser, K. Fennel, O. Schofield, and A. Sutton, "Monitoring ocean biogeochemistry with autonomous platforms," *Nature Reviews Earth & Environment*, vol. 1, no. 6, pp. 315–326, 2020.

[10] J. Vazquez-Cuervo, C. Gentemann, W. Tang, D. Carroll, H. Zhang, D. Menemenlis, J. Gomez-Valdes, M. Bouali, and M. Steele, "Using saildrones to validate arctic sea-surface salinity from the smap satellite and from ocean models," *Remote Sensing*, vol. 13, no. 5, p. 831, 2021.

[11] M. Chellapurath, K. L. Walker, E. Donato, G. Picardi, S. Stefanni, C. Laschi, F. Giorgio-Serchi, and M. Calisti, "Analysis of station keeping performance of an underwater legged robot," *IEEE/ASME Transactions on Mechatronics*, 2021.

[12] K. L. Walker, R. Gabl, S. Aracri, Y. Cao, A. A. Stokes, A. Kiprakis, and F. Giorgio-Serchi, "Experimental validation of wave induced disturbances for predictive station keeping of a remotely operated vehicle," *IEEE Robotics and Automation Letters*, vol. 6, no. 3, pp. 5421–5428, 2021.

[13] E. I. Sarda, H. Qu, I. R. Bertaska, and K. D. von Ellenrieder, "Station-keeping control of an unmanned surface vehicle exposed to current and wind disturbances," *Ocean Engineering*, vol. 127, pp. 305–324, 2016.

[14] P. Walters, R. Kamalapurkar, F. Voight, E. M. Schwartz, and W. E. Dixon, "Online approximate optimal station keeping of a marine craft in the presence of an irrotational current," *IEEE Transactions on Robotics*, vol. 34, no. 2, pp. 486–496, 2018.

[15] B. Li, B. R. Page, J. Hoffman, B. Moridian, and N. Mahmoudian, "Rendezvous planning for multiple auvs with mobile charging stations in dynamic currents," *IEEE Robotics and Automation Letters*, vol. 4, no. 2, pp. 1653–1660, 2019.

[16] E. Schlieben, "Skamp–an amazing unmanned sailboat," *Ocean Industry*, pp. 38–43, 1969.

[17] B. Smith, "Skamp–roboat boat with rigid sails patrols ocean beat," *Popular Science*, vol. 196, no. 5, pp. 70–72, 1970.

[18] G. H. Elkaim, "System identification for precision control of a wing-sailed gps-guided catamaran," Ph.D. dissertation, Stanford University, 2002.

[19] G. Elkaim and R. Kelbley, "Station keeping and segmented trajectory control of a wind-propelled autonomous catamaran," in *Proceedings of the 45th IEEE Conference on Decision and Control*. IEEE, 2006, pp. 2424–2429.

[20] C. Viel, U. Vautier, J. Wan, and L. Jaulin, "Position keeping control of an autonomous sailboat," *IFAC-PapersOnLine*, vol. 51, no. 29, pp. 14–19, 2018.

[21] W. Qi, Q. Sun, X. Ji, Y. Liang, Z. Cao, and H. A. Qian, "A kelvin wake avoidance scheme for autonomous sailing robots based on orientation-restricted dubins path," *IEEE Robotics and Automation Letters*, 2021.

[22] Z. Feng, J. Qiu, H. Liu, Q. Sun, N. Ding, Z. Sun, T. L. Lam, and H. Qian, "An adaptive position keeping algorithm for autonomous sailboats," in *2019 IEEE International Conference on Robotics and Biomimetics (ROBIO)*. IEEE, 2019, pp. 527–532.

[23] SailBot: https://www.sailbot.org/.

[24] WRSC: https://www.roboticsailing.org/.

[25] Microtransat Challenge: https://www.microtransat.org/.

[26] U. Vautier, C. Viel, J. Wan, L. Jaulin, R. Hone, and M. Dai, "Restricted orientation dubins path with application to sailboats," *IEEE Robotics and Automation Letters*, vol. 4, no. 4, pp. 4515–4522, 2019.

[27] H.-Y. Chen, Z. I. Bell, P. Deptula, and W. E. Dixon, "A switched systems approach to path following with intermittent state feedback," *IEEE Transactions on Robotics*, vol. 35, no. 3, pp. 725–733, 2019.

[28] W. Qi, Q. Sun, C. Liu, X. Ji, Z. Cao, Y. Liang, and H. Qian, "Collision risk assessment and obstacle avoidance control for autonomous sailing robots," in *2021 IEEE International Conference on Robotics and Automation (ICRA)*. IEEE, 2021, pp. 2511–2517.

[29] J. Melin, "Modeling, control and state-estimation for an autonomous sailboat," 2015.

[30] Q. Sun, W. Qi, X. Ji, and H. A. Qian, "V-stability based control for energy-saving towards long range sailing," *IEEE Robotics and Automation Letters*, 2021.